Pi-SAR X-BAND 영상에 의한 파랑 이미징 메커니즘 연구
OCEAN WAVE IMAGING MECHANISMS BY AIRBORNE SAR: Pi-SAR X-BAND

Chan-Su Yang
Senior Researcher, Ocean Satellite Research Group
Korea Ocean Research & Development Institute (KORDI)
1270 Sa2-dong Sangrokgu Ansan, Seoul 426-744 Korea
Tel: (82)-31-400-7678 Fax: (82)-31-400-7606
E-mail: yangcs@kordi.ac.kr

KEY WORDS: SAR, Wave, PiSAR, Velocity Bunching

ABSTRACT: In the present article, wave imaging mechanisms were investigated using airborne Pi-SAR (Polarimetric-Interferometric SAR) X-band VV images of ocean waves around the Miyake Island at approximately 180 km south from Tokyo, Japan. Two images of a same scene were produced at approximately 20 min. interval from two directions at right angles. One image shows dominant range travelling waves, but the other image shows a different wave pattern. This difference can be caused by the different image modulations of RCS and velocity bunching. In this study, 18 subimages are extracted, and the directional wave spectra are compared to each other of the two different areas.

1. INTRODUCTION

Analysis of ocean waves using synthetic aperture radar (SAR) images is an important issue in oceanography, not only for an academic interest but also for validation and improvement of wave forecasting models and for the utilization in shipping industry and in the field of maritime disaster prevention. Since the launch of the SEASAT satellite with a L-band SAR in 1978, considerable effort has been made to understand the SAR imaging mechanisms of ocean waves, and a large number of publications are available. Consequently, the principal mechanisms of imaging ocean waves by SAR are considered to be well understood. According to the present knowledge, there appear 4 major image modulations to contribute to SAR image formation of ocean waves [1]. The first is the RCS (Radar Cross Section) modulation which is largest for range travelling waves and vanishes for azimuth travelling waves. The second is the velocity bunching modulation arising from the wave motion. This modulation is inherent to SAR, and it is largest for azimuth waves and vanishes for range waves. The third and fourth are the tilt and hydrodynamic modulations associated with the small-scale waves. Among these modulations, velocity bunching still requires some attention, because its theory is not yet, in a strict sense, confirmed by experiment.

In the present article, we analyse airborne Pi-SAR (Polarimetric-Interferometric SAR) X-band images of ocean waves around the Miyake Island at approximately 180 km south from Tokyo, Japan. Two images of a same scene were produced at approximately 40 min. interval from two directions at right angles. One image shows dominant range travelling waves, but the other image shows a different wave pattern. This difference can be caused by the different image modulations of RCS and velocity bunching. We have estimated the dominant wavelength from the image of range waves, and from the wave phase velocity computed from the dispersion relation (though no wave height data were available), the image intensity is computed by using

the velocity bunching model [2]. The comparison of the result with the second image at right angle strongly suggests the evidence of velocity bunching.

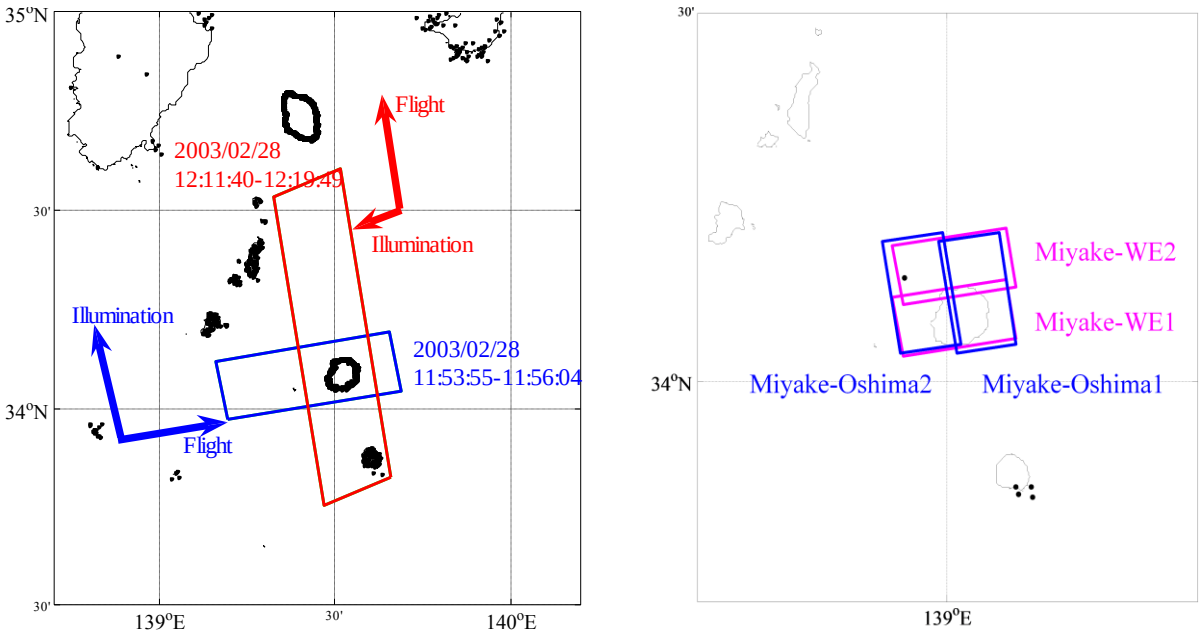

Fig. 1 Flight paths (left image) and research area (right) in and around Miyake-Oshima, Japan on Feburuary 28, 2004(left).

2. Pi-SAR System

Since 1995, National Institute of Information and Communications Technology (NICT) and Japan Aerospace Exploration Agency (JAXA) have collaborated to develop an airborne high-resolution multiparameter synthetic aperture radar. This synthetic aperture radar is a dual frequency radar operating at L-band and X-band frequencies with polarimetric functions. The X-band system also has an interferometric function by which topographic mapping of the ground surface is achieved. The development of the L-band and the X-band parts was carried out by JAXA and NICT, respectively.

Pi-SAR observes the ground surface using dual frequencies simultaneously with the X-band (λ =3.14 cm) and the L-band (λ =23.6 cm). The horizontal resolution is 1.5 m for the X-band and 3 m for the L-band, and it is capable of polarimetric observation (by transmitting/receiving horizontal and vertical polarized waves). Pi-SAR also had features for an interferometric function to provide elevation profiles of the ground using two antennas through X-band observations. Table 1 shows the major specifications of Pi-SAR.

For the polarimetric function, the X-band main-antenna is equipped to deal with both vertical and horizontal polarized waves. The sub-antenna, which is required for interferometry, employs vertically polarized waves, since the return power of these waves is relatively large. The two antennas should be firmly installed as far as possible because the fluctuations in the antenna's position, caused by airplane vibration, result in measurement errors. They are installed as shown in Figure 2, and antenna separation is 2.3 m in the Pi-SAR configuration. The roll angle is variable between 40 and 65 degree (peak to peak) to extend the range of incidence angle selectively for all target objects and observation modes. The dual-axis variable angle (within ±6.5 degree) mechanism control the yaw angle so that the antenna are kept parallel along the flight direction, regardless of the drift angle of the airplane.

Here, the SSC (single-look, slant range, complex) data are used.

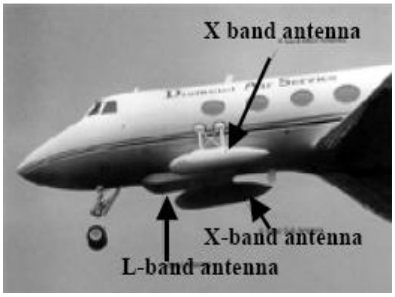

	X-band SAR			L-band SAR	
Center Frequency	9.55 GHz			1.27 GHz	
Peak Power	6.3 kW			3.0 kW	
Bandwidth	100 MHz			50 MHz	
Antenna (L×W)	1.05 m×0.19 m			1.55 m ×0.65 m	
Incidence Angle	10 to 75 degree variable			20 to 65 degree fix	
Observation Modes	2 CH Polarimetry or Interferometry	4 CH Polarimetry	6 CH Polarimetry and Interferometry	1 CH	4 CH Polarimetry
Swath Width (slant)	20.6/ 42.9 km	9.4/ 20.4 km	5.6/ 12.9 km	42.9 km	20.4 km
Range Resolution	1.5/ 3 m	1.5/ 3 m	1.5/ 3 m	3/ 5/ 10/ 20 m	3/ 5/ 10/ 20 m
Azimuth Resolution	1.5/ 3 m			3/ 6 m	
Interferometry Baseline	Cross-track 2.3 m			×	
Sampling frequency	123.45/ 61.725 MHz			61.7/ 30.9 MHz	

Fig. 2 Installed Pi-SAR system Table 1 Main characteristics of Pi-SAR system

3. Results and Discussion

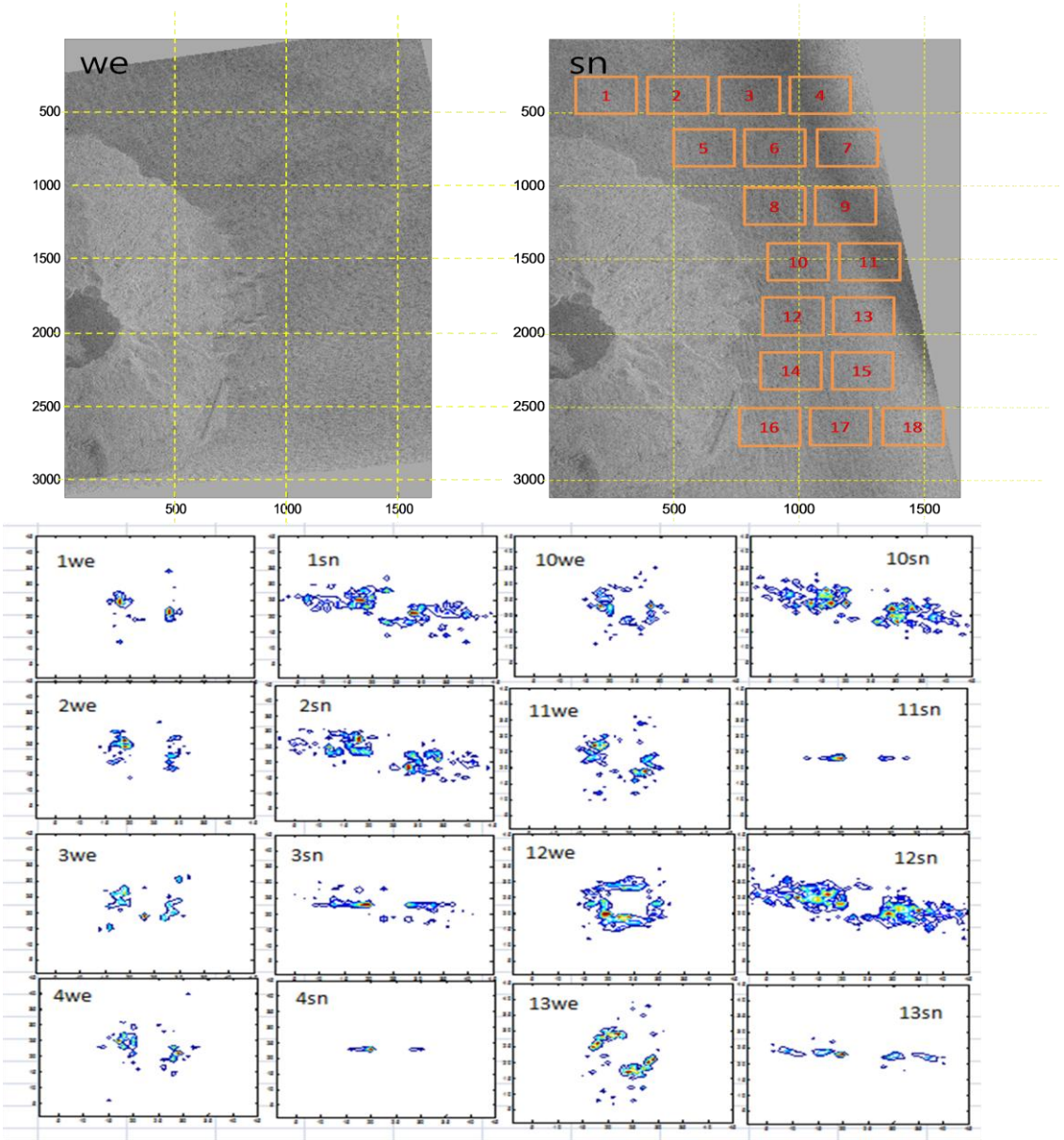

Fig. 3 Geo-corrected images (Top-left: Miyake-WE1, Top-right: Miyake-Oshima1) and directional wave spectra at each areas (bottom).

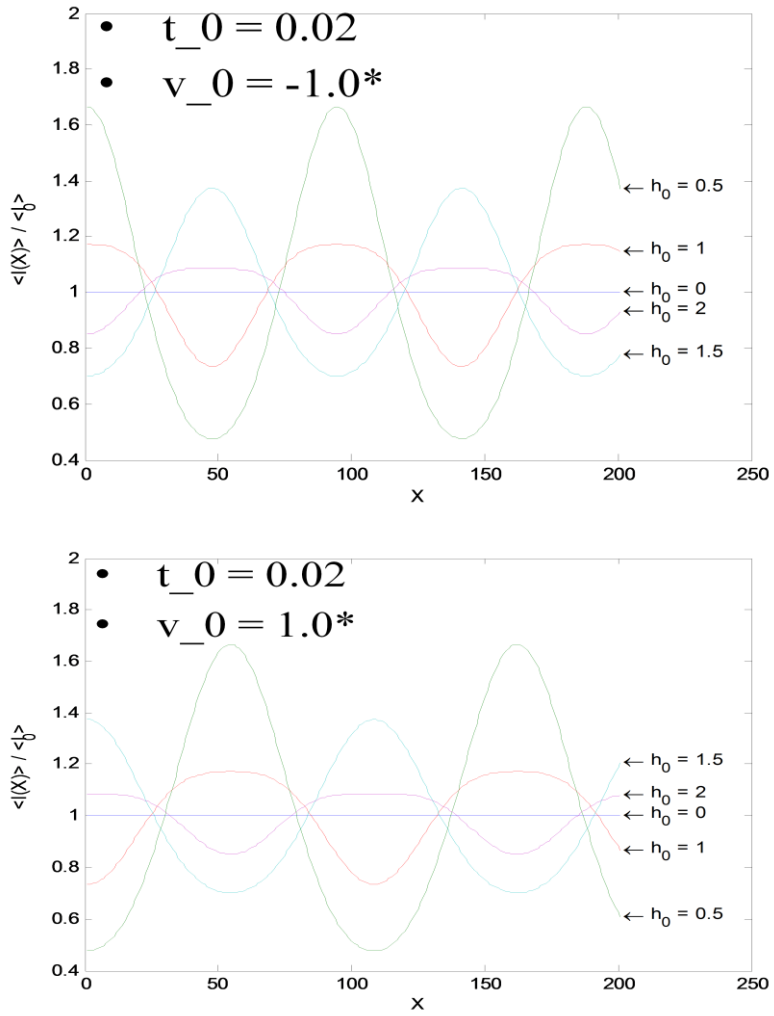

Fig. 4 Azimuth components of the SAR relative intensity of ocean waves modulated by velocity bunching. The ocean wave length is 100 m, wave directions for flight direction and its opposite, and wave height h0 for 1 to 2 m.

ACKNOWLEDGEMENTS

This work was supported by the Basic Research Project, "Development of Management and Restoration Technologies for Estuaries" of KORDI and the Public Benefit Project of Remote Sensing, "Satellite Remote Sensing for Marine Environment" of Korea Aerospace Research Institute.

References

[1] K. Hasselmann, R.K. Raney, W.J. Plant, W. Alpers, R.A. Shuchman, D.R. Lyzenga, C.L. Rufenach, and M.J. Tucker, "Theory of synthetic aperture radar ocean imaging: A MARSEN view," *J. Geophy. Res.*, vol. 90, no. C3, pp.4659-4686, 1985.

[2] K. Ouchi and D.A. Burridge, "Resolution of a controversy surrounding the focusing mechanisms of synthetic aperture radar images of ocean waves," *IEEE Trans. Geosci. Remote Sens.*, vol.32, pp.1004-1016, 1994.